CASSCF/CASPT2 Calculation of the Low-Lying Electronic States of the CH 3 Se Neutral Radical and Its Cation

RESEARCH · JUNE 2015

DOI: 10.13140/RG.2.1.1332.4969

CASSCF/CASPT2 Calculation of the Low-Lying Electronic States of the CH_3Se Neutral Radical and Its Cation

Ming-Xing Song, Zeng-Xia Zhao, Fu-Quan Bai, Yue-Jie Liu, Hong-Xing Zhang,* and Chia-chung Sun

Institute of Theoretical Chemistry, State Key Laboratory of Theoretical and Computational Chemistry, Jilin University, Changchun 130023, People's Republic of China

Received: March 15, 2010; Revised Manuscript Received: May 12, 2010

Electronic states of the CH_3Se and its cation CH_3Se^+ have been studied using the complete active space self-consistent field (CASSCF) and multiconfiguration second-order perturbation theory (CASPT2) methods in conjunction with the ANO-RCC(TZP) basis set. To investigate the Jahn−Teller effect on the CH_3Se radical, C_s symmetry was used for CH_3Se in calculations. The results show that the Jahn−Teller effect is very small (69 cm^{-1}) and the $1^2A'$ state is slightly more stable than the $1^2A''$ state (8 cm^{-1}). The CH_3Se has been found to have a $1^2A'$ ground state with a C−Se bond distance of 1.975 Å. The computed C−Se stretching $\nu_6(a')$ frequency is 554.1 cm^{-1}, which is in good agreement with the experimental values of 600 ± 60 cm^{-1}. The calculations for CH_3Se at 3.621 and 5.307 eV are attributed to $1^2A' \rightarrow 2^2A'(1^2A_1)$ and $1^2A' \rightarrow 2^2A''$, respectively. The vertical and adiabatic ionization energies were obtained to compare with the PES data.

Introduction

Due to their potential importance in atmospheric, environmental, and biological chemistry, selenium and its compounds have drawn considerable attention.[1−21] As the simplest organic selenium species, the CH_3Se radical is suggested to be an important intermediate in most chemical reactions of both dimethyl selenide and dimethyl diselenide, and it has to be included in the global selenium cycle.[22,23] Therefore, the theoretical investigation of the CH_3Se radical is very important work. The most thorough studies have been reported on the excitation spectroscopy and photoelectron spectroscopy of its homologous radicals, CH_3O and CH_3S;,[24−35] however, much less is known about CH_3Se.

Several studies by photoelectron spectroscopy (PES) were carried out that were mainly concerned with the vertical ionization of different molecule orbitals of CH_3Se. In a solely experimental study on CH_3Se, Sun et al.[36] obtained the CH_3Se radical through pyrolysis of $CH_3SeSeCH_3$; they reported six experimental energies in the low ionization energy region for CH_3Se. They also performed some limited ab initio calculations of the vertical ionization energies according to C_{3v} symmetry from the G2 and DFT methods to explain their findings for CH_3Se. However, the structures and properties of the ground and excited states that would be of importance in the neutral compounds and its cation (CH_3Se^+) were not studied and need to be further investigated. Moreover, besides the vertical ionization energies they calculated, adiabatic energies with geometric relaxation of the excited would be an important contribution to the ionization energies and to explain the characteristics of the electronic states.

It is noteworthy that all the previous theoretical and experimental studies were concerned with only the ground state of CH_3Se. So far, there has been no work addressing its excited states, experimentally or theoretically. In an effort to understand more about this radical, we have carried out a study on the low-lying electronic states of CH_3Se and CH_3Se^+ using the CASSCF/CASPT2 method, which is effective for theoretical studies of excited states of molecules.[37−43] We report the results for excited electronic states, including the predicted equilibrium geometries, harmonic vibrational frquencies, and adiabatic and vertical excitation energies.

Methodology

The geometries of the low-lying electronic states of CH_3Se radical and CH_3Se^+ cation have been investigated via the complete active space self-consistent field (CASSCF)[44] method and the ANO-RCC(TZP) basis set—a (14s, 9p, 4d, 3f, 2g) set contracted to (4s, 3p, 2d, 1f) for the C atom, a (20s, 17p, 11d, 4f, 2g) set contracted to (6s, 5p, 3d, 2f, 1g) for the Se atom, and a (8s, 4p, 3d, 1f) set contracted to (6s, 4p, 3d, 1f) for the H atom—and the ANO-RCC basis set—a (14s, 9p, 4d, 3f, 2g) set contracted to (8s, 7p, 4d, 3f, 2g) for the C atom, a (20s, 17p, 11d, 4f, 2g) set contracted to (9s, 8p, 6d, 4f, 2g) for the Se atom, and a (8s, 4p, 3d, 1f) set contracted to (6s, 4p, 3d, 1f) for the H atom.[45,46] Second-order perturbation (CASPT2)[47] calculations were performed to consider the dynamic correction, which takes the CASSCF wave functions as a reference in the second-order perturbation treatment. Scalar relativistic effects were included via a Douglas−Kroll (DK) Hamiltonian.[48,49] The Multiconfigurational linear response (MCLR)[50] was used to calculate the harmonic vibartional frequencies.

To investigate the distortion of the excited states of CH_3Se, all calculations were carried out in C_s symmetry, a subgroup of the C_{3v} point group to which CH_3Se belongs. The selection of the active space is a crucial step in a CASSCF/CASPT2 calculation. In probe SCF, the calculation of the electronic configuration of the neutral ground radical is confirmed as $[core](12a')^2(13a')^2(5a'')^2(14a')^2(15a')^2(6a'')^2(16a')^\alpha$, in which [core] denotes $(1a')^2(2a')^2(3a')^2(4a')^2(1a'')^2(5a')^2(6a')^2(7a')^2(8a')^2(2a'')^2(9a')^2(10a')^2(3a'')^2(11a')^2(4a'')^2$. All bonding and antibonding combinations of Se 4p were included in all calculations, thus giving 13 electrons in 11 orbitals, which means eight a′ orbitals and three a″ orbitals. The same active space was chosen

* .

10.1021/jp102321c
Published on Web 06/10/2010

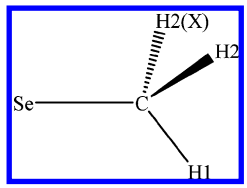

Figure 1. Molecular geometry of the CH_3Se radical and CH_3Se^+ cation.

for the CH_3Se^+, but the number of active electrons was decreased by one.

The CAS state interaction (CASSI)[51] method was employed to compute the transition dipole moments, which were combined with CASPT2 energy differences to obtain oscillator strengths.

The optimized geometry of the ground state of CH_3Se was used to calculate the vertical ionization energies, which are obtained from the difference of the total energies between the resulting radical ion and the neutral CH_3Se radical. The calculated adiabatic ionization energies are obtained from the difference of the total energies between the radical ion and the neutral CH_3Se radical in their respective optimized geometries. All the above calculations were performed with the MOLCAS 6.2[52] quantum chemistry software on SGI/O3900.

Results and Discussion

1. CASSCF/CASPT2 Results for the Ground and Excited States of CH_3Se. ***1.1. Equilibrium Structures.*** Geometries and atom labelings used for the CH_3Se radical and its cation are shown in Figure 1. According to the result of Sun et al.,[36] the ground state of the CH_3Se radical has E symmetry. The degeneracy of this state must induce a reduction of the C_{3v} symmetry under the Jahn−Teller effect. To determine the importance of this effect, we have calculated the ^2E state structure with a C_{3v} symmetry constraint, which then was relaxed.

Tables 1 and 2 exhibit the optimized geometries and energy separations for the ground state and low-lying electronic excited states of CH_3Se in C_{3v} and C_s symmetry at the CASSCF/CASPT2 level. As shown in Table 1, the predicted results by ANO-RCC(TZP) and ANO-RCC basis set calculations are very close, with the difference being less than 0.01 Å for bond length and 1.0° for angle. To keep a balance between the computation cost and computation precision, our analysis is done at the ANO-RCC(TZP) basis set and the results of the ANO-RCC basis set are also listed. Comparing the energetic values of CASSCF and CASPT2 indicated the dynamical electron correlation effect must be considered in calculations. The CASSCF calculations for the ^2E state of CH_3Se have been performed under C_s symmetry keeping the C_{3v} symmetry constraints. As predicted by the Jahn−Teller theorem, the C_{3v} symmetry nuclear configuration in the ^2E ground state of CH_3Se is expected to be unstable with no spin−orbit coupling included. There are two specific points on the adiabatic potential energy surface (PES) of CH_3Se corresponding to distorted nuclear configurations (a minimum and a saddle point).[53−55] That is, the ^2E state of CH_3Se would undergo Jahn−Teller distortion into the $1^2A'$ and $1^2A''$ states with C_s symmetry. The C_s ($1^2A'$) form is slightly more stable (8 cm^{-1}) than the C_s ($1^2A''$) one. The energy stabilization by the Jahn−Teller effect (ΔE_{J-T}) is very weak (69 cm^{-1}). Comparison of geometries optimized for the high-symmetry ^2E and for CH_3Se Jahn−Teller distorted structures shows that the largest deformations affect the HCSe bond angles. Thus, for the geometry of $1^2A'$, the $SeCH_1$ bond angle decreases by 2.5° and that for SeCH2(SeCH2(X)) increases by 1.3°. On the contrary, for the structure of $1^2A''$, the SeCH1 bond angle increases by 1.9° and that for SeCH2(SeCH2(X)) decreases by 1.1°.

The CASSCF frequency calculations produced no imaginary frequencies for the $1^2A'$ state, indicating that the CASSCF geometry of $1^2A'$ corresponds to energy minima in the respective potential energy surfaces (PESs). However, the CASSCF frequency calculations for the $1^2A''$ state produced one imaginary frequency in the a″ mode (568.3i), indicating that the CASSCF geometry of the $1^2A''$ state corresponds to a first-order saddle point in the PES. From the above analysis the lowest state $1^2A'$ is confirmed as the ground state of the CH_3Se neutral radical, whose electronic configuration can be described as $[core](12a')^2(13a')^2(5a'')^2(14a')^2(15a')^2(6a'')^2(16a')^\alpha$ with a coefficient of about 0.97, where [core] represents $(1a')^2(2a')^2$-$(3a')^2$ $(4a')^2(1a'')^2$ $(5a')^2(6a')^2(7a')^2(8a')^2(2a'')^2(9a')^2(10a')^2(3a'')^2$-$(11a')^2(4a'')^2$. The orbital plots of the CH_3Se are present in Figure 2. In the $1^2A'$ and $1^2A''$ states of CH_3Se, the unpaired electron resides in 16a′ and 6a″, respectively, between which the calculated orbital energy interval is very small. As can be seen, 16a′ and 6a″ are perpendicular to the C−Se bond and mostly composed of the $4p_y$ and the $4p_x$ orbitals of the Se atom, respectively.

We can see from the electronic configurations in Table 2 that $2^2A'(1^2A_1)$ can be taken as the result of promoting an electron from the highest occupied 15a′ orbital of the ground state to the half-filled 16a′, which has a dominant leading configuration $[core](12a')^2(13a')^2(5a'')^2(14a')^2(15a')^\alpha(6a'')^2(16a')^2$ with a coef-

TABLE 1: Optimized Structure for the Ground State and Excited States of CH_3Se Calculated at the CASSCF/CASPT2 Level of Theory with Two Basis Sets

	state	basis set	R_{CSe} (Å)	R_{CH1} (Å)	R_{CH2} (Å)	α_1 (deg)[a]	α_2 (deg)[a]	α_3 (deg)[a]	α_4 (deg)[a]	β_1 (deg)[a]	β_2 (deg)[a]
C_{3v}	1^2E	ANO-RCC(TZP)	1.977	1.100	1.100	109.2	109.2	109.7	109.7	120.0	120.0
		ANO-RCC	1.976	1.100	1.100	109.2	109.2	109.7	109.7	120.0	120.0
C_s	$1^2A'$	ANO-RCC(TZP)	1.975	1.103	1.099	106.7	110.5	109.1	110.8	118.5	123.0
		ANO-RCC	1.975	1.103	1.099	106.7	110.3	109.2	110.9	118.6	122.9
	$1^2A''$	ANO-RCC(TZP)	1.976	1.098	1.101	111.1	108.1	110.3	108.7	121.2	117.5
		ANO-RCC	1.977	1.098	1.101	111.1	108.1	110.3	108.8	121.2	117.6
	$2^2A'(1^2A_1)$	ANO-RCC(TZP)	2.334	1.092	1.092	97.9	97.9	118.0	118.0	120.0	120.0
		ANO-RCC	2.334	1.092	1.092	98.3	98.3	118.0	118.0	120.0	120.0
	$1^4A'$	ANO-RCC(TZP)	1.929	1.102	1.090	106.7	105.7	111.4	115.4	118.6	122.7
		ANO-RCC	1.936	1.102	1.088	106.3	106.3	111.3	114.7	118.7	122.6
	$2^2A''$	ANO-RCC(TZP)	2.016	1.100	1.226	121.8	122.3	106.5	62.5	142.1	75.8
		ANO-RCC	2.018	1.099	1.225	122.0	122.3	106.4	62.3	142.2	75.6

[a] α_1 represent the SeCH1 angle; α_2 represent the SeCH2 angle; α_3 represent the H1CH2 angle; α_4 represent the H2CH2(X) angle; β_1 represents the H2CSeH1 dihedral angle; β_2 represents the H2CSeH2(X) dihedral angle.

TABLE 2: Leading Configuration, CI Coeficient, Occupation, Adiabatic Excitation Energies (E_a), Vertical Excitation Energies (E_v), and Oscillator Strengths (f) of CH_3Se Calculated at the CASSCF/CASPT2/ANO-RCC(TZP) Level of Theory

state	configuration		E_a(CASSCF) (in eV)	E_a(CASPT2) (in eV)	E_v(CASSCF) (in eV)	E_v(CASPT2) (in eV)	f
	occupation[a]	coefficient					
$1^2A'$	$(15a')^2(6a'')^2(16a')^\alpha$	0.97	0.000	0.000	0.000	0.000	
$1^2A''$	$(15a')^2(6a'')^\alpha(16a')^2$	0.97	0.001	0.001	0.023	0.025	2.80×10^{-9}
$2^2A'(1^2A_1)$	$(15a')^\alpha(6a'')^2(16a')^2$	−0.97	3.104	3.210	3.699	3.621	5.97×10^{-3}
$2^2A''$	$(15a')^2(5a'')^2(6a'')^\alpha(16a')^2$	−0.71	6.143	5.830	5.909	5.307	5.56×10^{-3}
	$(15a')^2(5a'')^\alpha(6a'')^2(16a')^2$	0.63					
$1^4A'$	$(15a')^2(6a'')^\alpha(16a')^\alpha(7a'')^\alpha$	−0.98	6.723	6.531	7.161	6.771	$<10^{-10}$

[a] In active orbitals "α" represents a singly occupied orbital containing an electron with an up spin, "β" represents a singly occupied orbital containing an electron with a down spin. The common configuration [core]$(12a')^2(13a')^2(5a'')^2(14a')^2$ is not presented for every state.

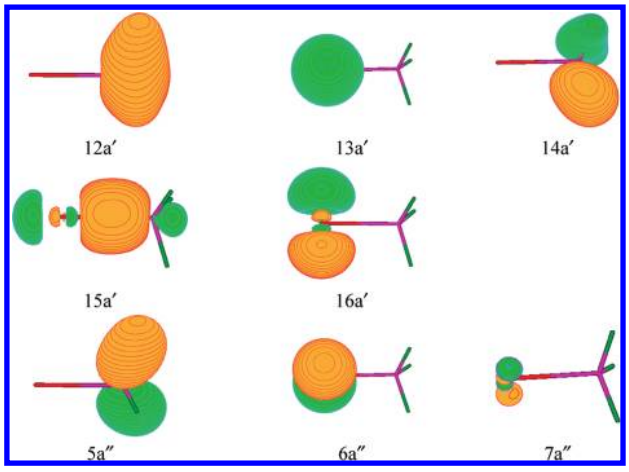

Figure 2. The plots of densities for some of the CH_3Se orbitals included in the active space.

ficient −0.97. Compared with the $1^2A'$ state, the C−Se bond length of $2^2A'$ is elongated by 0.359 Å. The 15a′ orbital is mostly of σ(C−Se) bonding character, consisting essentially of the $4p_z$ orbital from the selenium atom and the $2p_z$ orbital from the carbon atom. For the single electron transition 15a′ → 16a′, the electron is promoted from a bonding interaction to a nonbonding orbital and the bonding interaction between the C and Se atoms is badly impaired. The Jahn−Teller effect is not evident in the $2^2A'$ state, since it retains C_{3v} symmetry.

The $2^2A''$ excited states have been optimized by using the SA-CASSCF method and present the remarkable character of multiconfiguration, which is composed of the configuration [core]$(12a')^2(13a')^2(5a'')^2(14a')^2(15a')^2(6a'')^\alpha(16a')^2$ with a coefficient −0.71 accompanied by the configuration [core]$(12a')^2$-$(13a')^2(5a'')^\alpha(14a')^2(15a')^2(6a'')^2(16a')^2$ with a coefficient of 0.63. The 5a″ orbital is mainly of σ bonding character (σ(C−H2(H2(X)). The elongating of the C−H bond in the geometry of the $2^2A''$ state can be understood by realizing the bonding character between the C and H2(H2(X)) atom in the 5a″ MOs of the molecule. The Jahn−Teller effect is evident in this state, and β_1(H2CSeH1) and β_2(H2CSeH2(X)) are 142.1° and 75.8°, respectively.

Furthermore, we also calculated the quartet states of the CH_3Se radical, only the quartet excited state $1^4A'$ has a converged equilibrium geometry, which has a dominant leading configuration [core]$(15a')^2(6a'')^\alpha(16a')^\alpha(7a'')^\alpha$ with a coefficient of −0.98. In the $1^4A''$ state, the C−Se bond of CH_3Se ruptures and tends to decompose (to CH_3 + Se).

1.2. Harmonic Frequencies. After the geometry optimizations, the frequency analyses are also performed. In Table 3, we list the harmonic vibration frequency values corresponding to nine types of normal modes, in which ν_6(a′) is of the C−Se bond-stretching mode. The experimental frequency values for this vibrational mode in the ground state of CH_3Se was reported by Sun et al.[36] The calculated ν_6(a′) value in the ground state is in good agreement with the experimental values. Except for $1^2A''$, all of the frequencies are real, and the optimized electronic states are confirmed to be stationary points in respective potential energy surfaces. The alteration of frequencies is also consistent with the change of the geometries.

1.3. Vertical Transition. The computed vertical excitation energies at the CASSCF/CASPT2//ANO-RCC(TZP) levels are listed in Table 2 together with oscillator strengths (f). According to the Franck−Condon theory, all of the vertical calculations are performed based on the equilibrium geometry of the neutral ground state.

Among these electronic excitations, the $1^2A' \rightarrow {}^2A'$ and $1^2A' \rightarrow {}^2A''$ electronic excitation are allowed by the spin and dipole rules. Our calculated oscillator strengths (f) reflect exactly these selection rules. As shown in Table 2 the $1^2A' \rightarrow 1^2A''$, $1^2A' \rightarrow 2^2A'(1^2A_1)$, and $1^2A' \rightarrow 1^2A''$ transitions calculated at 0.025, 3.621, and 6.771 eV have oscillator strengths (f) of 2.80×10^{-9}, 5.97×10^{-3}, and 5.56×10^{-4}, respectively.

2. CASSCF/CASPT2 Results for the Ground and Excited State of CH_3Se^+. ***2.1. Equilibrium Structures of CH_3Se^+.*** Because CH_3Se^+ is the product from the photoelectron ionization of CH_3Se, the ground and excited states of CH_3Se^+ using the same basis sets and methods as the neutral molecules were calculated (Table 4). A total of 7 ionic states of CH_3Se^+ cations are optimized adiabatically, and the frequency analyses are also performed.

On the basis of adiabatic energies, the $1^3A''(1^3A_2)$ state is confirmed as the ground state of CH_3Se^+ cation, which has a dominant leading configuration [core] $(12a')^2(13a')^2(5a'')^2(14a')^2$-$(15a')^2(6a'')^\alpha(16a')^\alpha$ with a coefficient of −0.97. As compared to the neutral radical's electronic structure, this state can result from eliminating the single electron in the 6a″ orbital of the ground neutral radical. As shown in Table 5, the Jahn−Teller effect is not evident in the ground state, since it retains C_{3v} symmetry. We found in excited states the geometries are also little affected.

The absolute value of configuration coefficient for $1^3A''$, $1^1A''$, $1^3A'$, $2^3A''$, and $2^1A''$ is around 0.97, indicating a single-reference character of the respective states. The $1^1A'$ and $2^1A'$ excited states present the remarkable character of multiconfiguration, which shows that 6a″ and 16a′ of CH_3Se^+ in these states are degenerate orbitals. According to the vertical and adiabatic energies, $1^1A'$ and $1^1A''$, $1^3A'$ and $2^3A''$ states are degenerate states and correspond to 1^1E and 1^3E in C_{3v} symmetry, respectively. We predict a strong transition in the adabatic excitation spectrum of CH_3Se^+ at 2.905 eV, which belong to the $1^3A''$ $(1^3A_2) \rightarrow 1^3A'$, $2^3A''(1^3E)$ transiton.

TABLE 3: Harmonic Frequencies for the Ground and Excited States of CH_3Se Calculated by MCLR[a]

vibraitonal mode[a]	expt[b]	B3LYP[b]	B3P86[b]	B3PW91[b]	$1^2A'$	$1^2A''$	$2^2A'$	$1^4A'$
$\nu_1(a')$ (antisymmetric C−H stretching)					3012.7	3028.1	3169.1	3056.4
$\nu_2(a')$ (symmetric C−H stretching)					2934.9	2929.4	3003.7	2957.1
$\nu_3(a')$ (symmetric C−H bending)					1484.0	1505.5	1445.2	1474.7
$\nu_4(a')$ (CH_3 umbrella)					1294.7	1311.8	1056.9	1324.6
$\nu_5(a')$ (CH_3 rocking)					773.0	902.4	521.3	841.2
$\nu_6(a')$ (C−Se stretching)	600 ± 60	585.4	609.1	605.9	554.1	553.7	311.2	526.9
$\nu_7(a'')$ (out-plane antisymmetric C−H stretching)					3021.0	2976.1	3169.1	3156.3
$\nu_8(a'')$ (out-plane antisymmetric C−H bending)					1425.7	1484.1	1445.2	1167.6
$\nu_9(a'')$ (out-plane CH_3 rocking)					471.3	581.7*i*	521.2	845.1

[a] Our calculations are performed at the ANO-RCC(TZP)basis set. [b] The experimenal and theoretical values taken from ref 36, in which all calculations are perfomed at the 6-311++G(3df, 3pd) basis set level.

TABLE 4: Optimized Structure for the Ground State and Excited States of CH_3Se^+ Calculated at the CASSCF/CASPT2 Level

state	basis set	R_{CSe} (Å)	R_{CH1} (Å)	R_{CH2} (Å)	α_1 (deg)[a]	α_2 (deg)[a]	α_3 (deg)[a]	α_4 (deg)[a]	β_1 (deg)[a]	β_2 (deg)[a]
$1^3A''(1^3A_2)$	ANO-RCC(TZP)	1.958	1.102	1.102	107.1	107.1	111.8	111.8	120.0	120.0
	ANO-RCC	1.958	1.102	1.102	107.1	107.1	111.7	111.7	120.0	120.0
$1^1A'$	ANO-RCC(TZP)	1.936	1.105	1.105	107.5	107.7	111.3	111.4	119.9	120.2
	ANO-RCC	1.937	1.105	1.105	107.3	107.5	111.4	111.6	119.9	120.3
$1^1A''$	ANO-RCC(TZP)	1.946	1.081	1.104	107.8	106.9	112.0	110.8	120.6	118.8
	ANO-RCC	1.948	1.081	1.104	107.5	106.8	112.1	111.1	120.5	118.9
$2^1A'(2^1A_1)$	ANO-RCC(TZP)	1.921	1.108	1.108	107.8	107.8	111.1	111.1	120.0	120.0
	ANO-RCC	1.921	1.107	1.107	107.7	107.7	111.2	111.2	120.0	120.0
$1^3A'$	ANO-RCC(TZP)	2.369	1.097	1.095	94.2	96.6	118.7	119.6	119.5	120.9
	ANO-RCC	2.368	1.098	1.096	94.2	96.6	118.7	119.6	119.5	121.0
$2^3A''$	ANO-RCC(TZP)	2.369	1.095	1.097	97.1	95.0	119.3	118.4	120.4	119.1
	ANO-RCC	2.365	1.096	1.097	97.5	95.2	119.3	118.3	120.4	119.1
$2^1A''$	ANO-RCC(TZP)	2.334	1.095	1.097	98.5	96.0	118.9	118.0	120.5	119.1
	ANO-RCC	2.334	1.095	1.097	98.6	96.0	118.9	118.0	120.5	119.0

[a] α_1 represents the SeCH1 angle; α_2 represents the SeCH2 angle; α_3 represents the H1CH2 angle; α_4 represents the H2CH2(X) angle; β_1 represents the H_2CSeH_1 dihedral angle; β_2 represents the H2CSeH2(X) dihedral angle.

TABLE 5: Leading Configuration, CI Coeficient, Occupation, Adiabatic Excitation Energies (E_a), Vertical Excitation Energies (E_v) and Oscillator Strengths (f) of CH_3Se^+ Calculated at the CASSCF/CASPT2/ANO-RCC(TZP) Level of Theory

	configuration						
state	occupation	coefficient	E_a(CASSCF) (in eV)	E_a(CASPT2) (in eV)	E_v(CASSCF) (in eV)	E_v(CASPT2) (in eV)	f
$1^3A''(1^3A_2)$	$(15a')^2(6a'')^\alpha(16a')^\alpha$	−0.97	0.000	0.000	0.000	0.000	
$1^1A'$	$(15a')^2(6a'')^0(16a')^2$	−0.69	1.341	1.029	1.346	1.069	$<10^{-10}$
	$(15a')^2(6a'')^2(16a')^0$	0.69					
$1^1A''$	$(15a')^2(6a'')^\beta(16a')^\alpha$	−0.97	1.289	1.202	1.346	1.069	
$2^1A'(2^1A_1)$	$(15a')^2(6a'')^2(16a')^0$	0.68	2.202	2.034	2.212	2.093	$<10^{-10}$
	$(15a')^2(6a'')^0(16a')^2$	0.68					
$1^3A'$	$(15a')^\alpha(6a'')^2(16a')^\alpha$	0.98	2.716	2.905	3.388	3.332	0.005
$2^3A''$	$(15a')^\alpha(6a'')^\alpha(16a')^2$	0.98	2.716	2.905	3.388	3.332	0.005
$2^1A''$	$(15a')^\alpha(6a'')^\beta(16a')^2$	0.97	3.328	3.650	4.017	4.135	$<10^{-10}$

The calculated harmonic frequencies for ionic states are summarized in Table 6. The CASSCF frequency calculations produced no imaginary frequencies for $1^3A''(1^3A_2)$, $1^1A'$, $1^1A''$, $2^1A'$, and $1^3A'$ states, indicating that the geometries of these states correspond to energy minima in the respective potential energy surfaces (PESs). The frequency calculations for $2^3A''$ and $2^1A''(2^1A_1)$ states produce one imaginary frequency (460.4*i* and 572.3*i*) in the a'' mode, indicating that the geometries of these states correspond to a first-order saddle point in the respective PESs.

2.2. Ionization Potentials of the CH_3Se Neutral Radical. There has been one photoelectron spectra experimental and calculation report about CH_3Se,[36] however; the calculations were only emphasized on the vertical ionization energies. We calculated the adiabatic ionization energies and vertical ionization energies which are summarized in Table 7, and that further proved our findings. The results of calculations with DFT are also reported in Table 7. Our calculated ionization potentials of CH_3Se are compared with those from experimental photoelectron spectroscopy. The values of VIP are consistent with that of experiment and DFT.[36] The difference between the vertical and adiabatic first ionization energy of CH_3Se is only 0.055 eV, which means that the 6a'' of the CH_3Se radical is a nonbonding orbital.

3. CH_3O and CH_3S Compared with Their Homologous Radicals. The Jahn−Teller stabilization energies (ΔE_{J-T}) and first vertical ionizsation energy (VIP) comparisons among the methoxy family radicals CH_3X (X = O, S, and Se) are also provided in Table 8. The oxygen atom is a second row element, the sulfur atom is a third row element, and the selenium is a fourth row element. The spin−orbital couplings in the system increase as the atomic weight of X increases.[56] Because the spin−orbit couplings can quench the ΔE_{J-T},[57] our calculated ΔE_{J-T} values decrease as follows: $\Delta E_{J-T}(CH_3Se) < \Delta E_{J-T}(CH_3S) < \Delta E_{J-T}(CH_3O)$. In our calculations the first VIP

TABLE 6: Harmonic Frequencies for the Ground and Excited States of CH_3Se^+ Calculated by MCLR in Conjunction with ANO-RCC(TZP) Basis Set

vibraitonal mode	$1^3A''(1^3A_2)$	$1^1A'$	$1^1A''$	$2^1A'$	$1^3A'$	$2^3A''$	$2^1A''(2^1A_1)$
$\nu_1(a')$ (antisymmetric C−H stretching)	3033.2	2949.8	3225.5	2979.3	3138.4	3152.9	3144.9
$\nu_2(a')$ (symmetric C−H stretching)	2923.7	2889.1	2931.5	2863.8	2964.7	2964.3	2957.5
$\nu_3(a')$ (symmetric C−H bending)	1442.0	1351.8	1436.7	1404.9	1470.6	1415.2	1438.3
$\nu_4(a')$ (CH_3 umbrella)	1289.6	1271.6	1307.9	1248.2	1196.2	1191.3	1168.1
$\nu_5(a')$ (CH_3 rocking)	801.3	517.3	811.7	792.6	521.5	560.5	476.7
$\nu_6(a')$ (C−Se stretching)	513.6	532.9	524.8	550.6	273.2	273.8	310.1
$\nu_7(a'')$ (out-plane antisymmetric C−H stretching)	3033.2	1453.8	2811.7	2979.3	3114.4	3078.3	3061.5
$\nu_8(a'')$ (out-plane antisymmetric C−H bending)	1442.0	1411.9	1453.4	1404.9	1321.6	1312.7	1332.4
$\nu_9(a'')$ (out-plane CH_3 rocking)	801.3	681.0	667.9	792.6	207.8	460.4i	572.3i

TABLE 7: Aiabatic and Vertical Ionization Potentials (AIP and VIP)

State	AIP	VIP	DFTa	expt[a]
$1^3A''(1^3A_2)$	8.603	8.658	8.840	8.78
$1^1A''$	9.632	9.713	9.272	9.26
$1^1A'$	9.805	9.717		
$2^1A'$	10.637	10.746	9.903	9.71
$1^3A'$	11.509	11.972	12.052	12.19
$2^3A''$	11.509	11.995		
$3^1A'$		12.775	12.418	
$2^1A''(2^1A_1)$	12.253	12.795		
$3^1A''$		14.478		
$3^3A''$		14.702	14.894	14.76
$4^1A'$		15.101	15.142	15.11

[a] The experimenal and theoretical values were taken from ref 36.

TABLE 8: The Jahn−Teller Stabilization Energies (ΔE_{J-T}) and First Vertical Ionization Potentials (IP) of the Methoxy Family Radicals (CH_3O, CH_3S, and CH_3Se)

species	ΔE_{J-T} (in cm^{-1})	VIP (in eV)	expt (in eV)
CH_3O	270[a]	10.791[c]	10.78[c]
CH_3S	92[a]	9.266[c]	9.26[c]
CH_3Se	69[b]	8.658[b]	8.78[d]

[a] The calculated values taken from ref 33. [b] This work. [c] The values taken from ref 34. [d] The values taken from ref 36.

of the CH_3Se is located lower than that of CH_3O and CH_3Se, and the final first VIP order is VIP(CH_3Se) < VIP(CH_3S) < VIP(CH_3O).

Conclusion

Systemic high-level ab initio calculations were performed to study and characterized several electronic states of CH_3Se and its cation by using ANO-RCC(TZP) basis sets and CASSCF/CASPT2 methods.

We predict the geometries of several states of CH_3Se. The $1^2A'$ state is confirmed as the ground state of CH_3Se. The CASSCF/MLCR frequency calculations predict the C−Se stretching $\nu_6(a')$ frequency is 554.1 cm^{-1}, which accords with the experimental values of 600 ± 60 cm^{-1}. Except for the $2^2A''$ state of CH_3Se, the Jahn−Teller effect is not evident. The calculated vertical transition energies of 0.025, 3.621, and 5.307 eV are attributed to the $1^2A' \rightarrow 1^2A''$, $1^2A' \rightarrow 2^2A'(1^2A_1)$, and $1^2A' \rightarrow 1^2A''$ transitions, respectively.

Theoretical studies for the ionization energies of CH_3Se are compared with the experimental PES data. We predicted a strong transition in the adiabatic excitation spectrum of CH_3Se^+ at 2.905 eV. In the methoxy family radicals CH_3X (X = O, S, and Se), the first vertical ionization energies (VIP) and the Jahn−Teller stabilization energies (ΔE_{J-T}) are smaller as the atomic weight of X increases.

Acknowledgment. This work was supported by the Natural Science Foundation of China (Grant No. 20973076).

References and Notes

(1) Rovira, M.; Giménez, J.; Martínez, M.; Martínez-Lladó, X. *J. Hazard. Mater.* **2008**, *150*, 279.
(2) Painter, E. P. *Chem. Rev.* **1941**, *28*, 179.
(3) Combs, G. F., Jr.; Combs, S. B. *The role of selenium in nutrition*; Academic Press: New York., 1986.
(4) Surai, P. F. *Selenium in Nutrition and Health*; Nottingham University Press: Nottingham, U.K., 2006.
(5) Hatfield, D.; Berry, M.; Gladyshev, V. *Selenium: Its Molecular Biology and Role in Human Health*; Springer: New York, 2006.
(6) Ip, C. *J. Nutr.* **1998**, *128*, 1845.
(7) Ganther, H. E. *Carcinogenesis* **1999**, *20*, 1657.
(8) Medina, D.; Thompson, H.; Ganther, H.; Ip, C. *Nutr. Cancer* **2001**, *40*, 12.
(9) Ip, C.; Dong, Y.; Ganther, H. E. *Cancer Metastasis Rev.* **2002**, *21*, 281.
(10) Diwadkar-Navsariwala, V.; Diamond, A. M. *J. Nutr.* **2004**, *134*, 2899.
(11) Rayman, M. P. *Proc. Nutr. Soc.* **2005**, *64*, 527.
(12) Lü, J.; Jiang, C. *Antioxid. Redox Signaling* **2005**, *7*, 1715.
(13) Davis, C. D.; Irons, R. *Curr. Nutr. Food Sci.* **2005**, *1*, 201.
(14) Hatfield, D. L.; Carlson, B. A.; Xu, X. M.; Mix, H.; Gladyshev, V. N. *Prog. Nucleic Acid Res. Mol. Biol.* **2006**, *81*, 97.
(15) Brigelius-Flohé, R. *Chem. Biodiversity* **2008**, *5*, 389.
(16) Whanger, P. D. *J. Trace Elem. Electrolytes Health Dis.* **1992**, *6*, 209.
(17) Moreno, P.; Quijano, M. A.; Gutièrrez, A. M.; Pèrez-Conde, M. C.; Càmara, C. *Anal. Chim. Acta* **2004**, *524*, 315.
(18) Arthur, J. R.; Nicol, F.; Beckett, G. J. *Biol. Trace Elem. Res.* **1992**, *33*, 37.
(19) *Nutr. Rev.* **1976**, *34*, 347.
(20) *J. Am. Diet. Assoc.* **1977**, *70*, 249.
(21) Kamel, A. H.; Elnaby, E. H.; Kelany, A. E. *Electroanalysis* **2008**, *20*, 1016.
(22) Chasteen, T. G.; Bentley, R. *Chem. Rev.* **2003**, *103*, 1. Dungan, R. S.; Yates, S. R.; Frankenberger, W. T. *Environ. Microbiol.* **2003**, *5*, 287. Amouroux, D.; Liss, P. S.; Tessier, E.; Hamren-Larsson, M.; Donard, O. F. X. *Earth Planet. Sci. Lett.* **2001**, *189*, 277.
(23) Groner, P.; Gillies, C. W.; Gillies, J. Z.; Zhang, Y.; Block, E. J. *Mol. Spectrosc.* **2004**, *226*, 169. Meija, J.; Beck, T. L.; Caruso, J. A. *J. Am. Soc. Mass. Spectrom.* **2004**, *15*, 1325.
(24) Callear, A. B.; Dickson, D. R. *Trans. Faraday Soc.* **1970**, *67*, 1987.
(25) Fournier, R.; DePrito, A. E. *J. Chem. Phys.* **1992**, *96*, 1183.
(26) Janousek, B. K.; Brauman, J. I. *J. Chem. Phys.* **1980**, *72*, 694.
(27) Ohbayashi, K.; Akimoto, H.; Tanaka, I. *Chem. Phys. Lett.* **1977**, *52*, 47.
(28) Engelking, O. C.; Ellison, G. B.; Lineberger, W. C. *J. Chem. Phys.* **1978**, *69*, 1826.
(29) Janousek, B. K.; Brauman, J. I. *J. Chem. Phys.* **1980**, *72*, 694.
(30) Gillbro, T. *Chem. Phys.* **1974**, *4*, 476.
(31) Jacox, M. E. *Can. J. Chem.* **1983**, *61*, 1036.
(32) Suzuki, M.; Inoue, G.; Akimoto, H. *J. Chem. Phys.* **1984**, *81*, 5405.
(33) Zhu, X. J.; Ge, M. F.; Wang, J.; Sun, Z.; Wang, D. X. *Angew. Chem.* **2000**, *112*, 2016.
(34) Wang, J.; Sun, Z.; Zhu, X. J.; Yang, X. J.; Ge, M. F.; Wang, D. X. *Angew. Chem., Int. Ed.* **2001**, *40*, 3055.

(35) Marenich, A. V.; Boggs, J. E. *Int. J. Quantum Chem.* **2006**, *106*, 2609.

(36) Sun, Q.; Li, Z.; Zeng, X.; Wang, W.; Sun, Z.; Ge, M.; Wang, D.; Mok, D. K. W.; Chau, F. *Chem. Phys. Chem.* **2005**, *6*, 2032.

(37) Hou, C. Y.; Zhang, H. X.; Sun, C. C. *J. Phys. Chem. A* **2006**, *110*, 10260.

(38) Hou, C. Y.; Zheng, Q. C.; Zhao, Z. X.; Zhang, H. X. *J. Phys. Chem. A* **2007**, *111*, 12037.

(39) Wei, Z. Z.; Li, B. T.; Zhang, H. X.; Sun, C. C.; Han, K. L. *J. Comput. Chem.* **2007**, *28*, 467.

(40) Li, B. T.; Wei, Z. Z.; Zhang, H. X.; Sun, C. C. *J. Phys. Chem. A* **2006**, *110*, 10643.

(41) Zhao, Z. X.; Zhang, H. X.; Sun, C. C. *J. Phys. Chem. A* **2008**, *112*, 12125.

(42) Zhao, Z. X.; Hou, C. Y.; Shu, X.; Zhang, H. X.; Sun, C. C. *Theor. Chem. Acc.* **2009**, *124*, 85.

(43) Liu, Y. J.; Zhao, Z. X.; Zhang, H. X.; Sun, C. C. *Theor. Chem. Acc.* **2010**, *125*, 65.

(44) Roos, B. O. In *Advance in Chemical Physica; Ab Initio Methods in Quantum Chemistry-II*; Lawley, K. P., Ed.; John Wiley & Sons: Chichester, England, 1987; Chapter 69, p 399.

(45) Widmark, P.-O.; Malmqvist, P.-Å.; Roos, B. O. *Theor. Chim. Acta* **1990**, *77*, 291.

(46) Roos, B. O.; Lindh, R.; Malmqvist, P.-Å; Veryazov, V.; Widmark, P.-O. *J. Phys. Chem. A* **2004**, *108*, 2851.

(47) Andersson, K.; Malmqvist, P.; Roos, B. O.; Sadlej, A. J.; Wolinski, K. *J. Phys. Chem.* **1990**, *94*, 5483.

(48) Hess, B. A. *Phys. Rev. A* **1985**, *32*, 756.

(49) Hess, B. A. *Phys. Rev. A* **1986**, *33*, 3742.

(50) McKellar, A. R. W.; Bunker, P. R.; Sears, T. J.; Evenson, K. M.; Saykally, R. J.; Langhoff, S. R. *J. Chem. Phys.* **1983**, *79*, 5251.

(51) Malmqvist, P. Å.; Roos, B. O. *Chem. Phys. Lett.* **1989**, *155*, 189.

(52) Karlström, G.; Lindh, R.; Malmqvist, P.-Å.; Roos, B. O.; Ryde, U.; Veryazov, V.; Widmark, P.-O.; Cossi, M.; Schimmelpfennig, B.; Neogrady, P.; Seijo, L. *Comput. Mater. Sci.* **2003**, *28*, 222.

(53) Höper, U.; Botschwina, P.; Köppel, H. *J. Chem. Phys.* **2000**, *112*, 4132.

(54) Barckholtz, T. A.; Miller, T. A. *J. Phys. Chem. A* **1999**, *103*, 2321.

(55) Aleksandr, V. M.; James, E. B. *J. Phys. Chem. A* **2004**, *108*, 10594.

(56) Igor, V. K.; Yuri, A. S.; Nicholas, J. T. *Chem. Rev.* **1993**, *93*, 537.

(57) Barckholtz, T. A.; Miller, T. A. *Int. Rev. Phys. Chem.* **1998**, *17*, 435.

JP102321C